

RESEARCH ARTICLE

Prospective scintillation electron detectors for S(T)EM based on garnet film scintillators

Petr Schauer¹  | Ondřej Lalinský¹ | Miroslav Kučera²¹Institute of Scientific Instruments of the CAS, Brno, Czech Republic²Charles University, Faculty of Mathematics and Physics, Prague, Czech Republic**Correspondence**Petr Schauer, Institute of Scientific Instruments of the CAS, Královopolská 147, Brno, Czech Republic.
Email: petr@isibrno.cz**Funding information**

Akademie Věd České Republiky, Grant/Award Number: RVO:68081731; European Commission, Grant/Award Number: CZ.1.05/2.1.00/01.0017; Grantová Agentura České Republiky, Grant/Award Numbers: GA16-05631S, GA16-15569S; Ministry of Education, Youth and Sports of the Czech Republic, Grant/Award Number: LO1212

Abstract

The performance of a scintillation electron detector for a scanning electron microscope and/or a scanning transmission electron microscope (S(T)EM) based on new epitaxial garnet film scintillators was explored. The LuGAGG:Ce and LuGAGG:Ce,Mg film scintillators with chemical formula $(\text{Ce}_{0.01}\text{Lu}_{0.27}\text{Gd}_{0.74})_{3-w}\text{Mg}_w(\text{Ga}_{2.48}\text{Al}_{2.46})\text{O}_{12}$ were prepared and their cathodoluminescence (CL) and optical properties were studied and compared with the properties of current standard bulk single crystal YAG:Ce and YAP:Ce scintillators. More specifically, CL decay characteristics, CL emission spectra, CL intensities, optical absorption coefficients, and the refractive indices of the mentioned scintillators were measured. Furthermore, electron interaction volumes with absorbed energy distributions, photomultiplier (PMT) photocathode matchings, modulation transfer functions (MTF), and the photon transport efficiencies of scintillation detectors with the mentioned scintillators were calculated. A CL decay time for the LuGAGG:Ce,Mg film scintillator as low as 28 ns with an afterglow of only 0.02% at 1 μs after the e-beam excitation was observed. As determined from calculated MTFs, the scintillation detectors with the new film scintillators lose contrast transfer ability above 0.6 lp/pixel, while the currently commonly used YAG:Ce single crystal scintillators already do so above 0.1 lp/pixel. It was also calculated that the new studied film scintillators have an 8% higher photon transfer efficiency, even for a simple disk shape compared with the standard bulk single crystal YAG:Ce scintillator. The studied LuGAGG:Ce,Mg epitaxial garnet film scintillators were evaluated as prospective fast scintillators for electron detectors, not only in S(T)EM but also in other e-beam devices.

KEYWORDS

cathodoluminescence, electron detector, LuGAGG:Ce,Mg, multicomponent garnet film, scintillator, SEM, STEM

1 | INTRODUCTION

Any detector is valuable if it does not waste the collected signal, does not introduce a noise, and its response is sufficiently fast. The important indicator of image quality is the modulation transfer function (MTF), which describes the ability to show fine image details. Using a scanning imaging system with a scintillation electron detector, the detector bandwidth, which is given specifically by the scintillator time response, is the key to a good MTF. Similarly important parameters are those that affect the detective quantum efficiency (DQE), which is primarily a measure of image noise. Efficient components with a high bandwidth and dynamic range are the key to a high DQE. To find the weaknesses of a scintillation detection system, one must examine the whole detection path step by step. Figure 1 shows an outline of a

scintillation detector for a scanning electron microscope and/or a scanning transmission electron microscope (S(T)EM). In fact, only three parameters of currently used standard scintillation electron detectors for S(T)EM can be referred as weaknesses in the system. Above all, the detector's weaknesses are (1) the electron-photon conversion efficiency; (2) the corresponding time response in the photon-generation step, and (3) the photon transport efficiency. The photon transport takes place in the steps of photon absorption in and escape from the scintillator, in the steps of photon coupling to and absorption in the light guide (LG), and finally also in the step of photon escape from the LG.

Photon generation (i.e., energy conversion) in the scintillator – more precisely: conversion from electrons to photons – is the most important detection process in S(T)EM. Physically, this is the

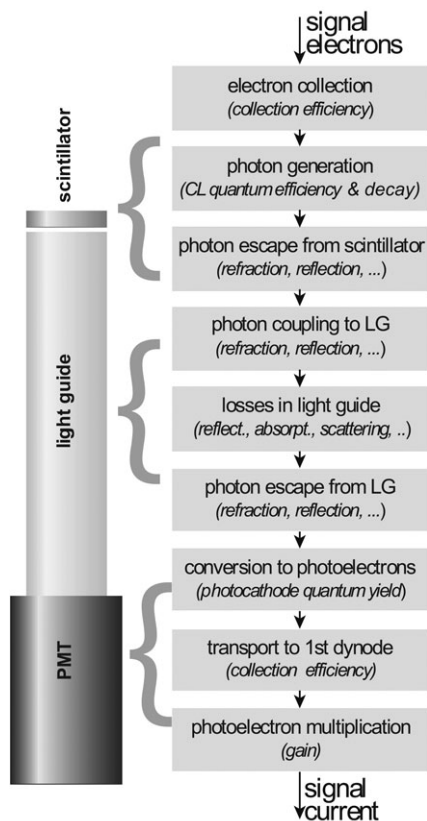


FIGURE 1 The detection path of a scintillation detector for S(T)EM. The important quantities of each step are in italics

phenomenon of cathodoluminescence (CL), and the determining physical quantities of this process are mainly the CL efficiency, the CL decay time and the CL afterglow. Cerium activated yttrium aluminum garnet (YAG:Ce – $\text{Y}_3\text{Al}_5\text{O}_{12}:\text{Ce}$) and the more expensive yttrium aluminum perovskite (YAP:Ce – $\text{YAlO}_3:\text{Ce}$) single crystal scintillators with well-defined properties are usually utilized in S(T)EM scintillation electron detectors to convert electron–photons. Much attention has been paid to the examination of their conversion efficiency, their time response, and their spectral characteristics (Aurata & Schauer, 1995). The theoretical limits of the conversion efficiency are about 23 and 25 photons per 1 kV electron (p/keV) for YAG:Ce and YAP:Ce, respectively. Unfortunately, there is no opportunity to improve the conversion efficiency if the values of 19 and 18 p/keV were obtained for YAG:Ce and YAP:Ce, respectively (Schauer, 1982). The reason is that the theoretical limits can never be achieved because they are calculated for ideal crystals, but it is practically impossible to produce these scintillators without impurities and defects. Rather, improvement of the decay characteristics of these single crystals can be expected.

In order to obtain a high-quality image in real time, the scintillation electron detector in the S(T)EM must possess a good MTF. In such a case, it is usually necessary to process each pixel in less than 100 ns without a loss of contrast (Bok & Schauer, 2014b). To meet this requirement, the detector must be equipped with a very fast scintillator that has a short decay time (decay to a value of $1/e$, where e is the base of natural logarithms) and a low afterglow even at a microsecond time range after an excitation. A scintillator with a long decay time causes an image blur and a scintillator with a high afterglow

reduces the image contrast in S(T)EM. However, in the current S(T)EM scintillation electron detectors, Czochralski-grown single-crystal scintillators, such as YAG:Ce and YAP:Ce, are commonly used today (Aurata, Schauer, Kvapil, & Kvapil, 1978, 1983a, 1983b, 1983c; Schauer, 2011). Unfortunately, most of these scintillators have a decay time that is too long (even longer than 100 ns for the YAG:Ce), and, even worse, they have a relatively high afterglow after the end of excitation (sometimes about 1% at 1 μs after the excitation). This is a consequence of the existence of shallow electron traps and Ce^{3+} ions, which are responsible for the delayed radiative emission and for luminescence quenching in the standard bulk Czochralski-grown single-crystal garnets (Chewpraditkul et al., 2009; Nikl et al., 2007, 2013; Nikl & Yoshikawa, 2015).

Single crystalline epitaxial garnet films activated with cerium show a great improvement in the decay characteristics compared with YAG:Ce single crystals (Kucera et al., 2016). In these garnet films, the mentioned influence of shallow traps and the ionization-induced quenching of the Ce^{3+} excited state is suppressed, which has a positive influence on the decay characteristics, including the substantial reduction of the afterglow. The GAGG:Ce ($\text{Gd}_3\text{Al}_5\text{-xGa}_x\text{O}_{12}:\text{Ce}$) single crystalline epitaxial films have also been studied as prospective scintillators in S(T)EM (Bok et al., 2016). Recently, the CL properties of the Mg^{2+} co-doped LuGAGG:Ce multicomponent single crystalline epitaxial garnet films were studied using a 10 keV collimated e-beam (Schauer, Lalinsky, Kucera, Lucenicova, & Hanus, 2017). The positive effect of Mg co-doping is evident in these scintillators, because their particularly low CL afterglow (0.02% at 1 μs or 0.01% at 2 μs after e-beam excitation) is by far the best value ever reported for garnets. A certain risk, but also an advantage in the application of these films, is their relatively small thickness, which requires the verification of interaction volume sizes in specific excitation modes. All of this is the reason to evaluate these single crystalline epitaxial garnet films for their use as prospective scintillators in the scintillation electron detectors for S(T)EM. This will be assessed in this work.

Photon transport in the scintillation electron detector for S(T)EM is only rarely examined when a scintillation electron detector is evaluated (Danilatos, 2012; Filippov, Rau, Sennov, Boyde, & Howell, 2001; Hibino, Irie, Aurata, & Schauer, 1992; Schauer, 2007; Schauer & Aurata, 1979, 1992; Yamamoto, Tanji, Hibino, Schauer, & Aurata, 2000). However, it has the prospect of improvement. Photons generated at the luminescent centers of a scintillator must be efficiently guided toward a photocathode of a PMT. During this stage of signal processing, significant losses can occur when the photons escape from the scintillator, are coupled to and transported through the light guide (LG), and when the photons escape from the LG and enter an entrance window of the PMT, as shown in Figure 1. The optimal choice of scintillator and LG materials, and the design of the system (often limited by the space available in the microscope chamber) can fundamentally affect the efficiency of the entire scintillation electron detector in S(T)EM (Schauer, 2007). Above all, optimizing the component coupling and the shape of the system can hardly be done without an optical analysis. Several decades ago, analytical calculations were preferred (Carrier & Lecomte, 1990; Keil, 1970). But computer technologies are currently at such a level that Monte Carlo (MC) simulations are no longer time consuming and they are used (Schauer, 2007; Schauer &

Autrata, 1992). The MC simulation enables researchers to get results easily for almost any scintillation detection system, even when many dimensions and many optical parameters are changed. In addition, the MC simulation does not depend on the symmetry of the simulated systems, and if one can restrict the simulation to rotationally symmetric detection systems, the photon transport in the detector can be expressed in a quite simple way. An assessment of the electron detector with the new scintillation garnet film in terms of the photon transport efficiency will also be done in this article.

2 | MATERIALS AND METHODS

2.1 | Garnet scintillators

Two scintillators based on epitaxial Ce^{3+} doped (Mg^{2+} undoped and Mg^{2+} co-doped, respectively) lutetium gadolinium aluminum gallium garnet films ($\text{LuGAGG}:\text{Ce},(\text{Mg})$) were prepared for the study in this article. The chemical formula of both scintillators is $(\text{Ce}_{0.01}\text{Lu}_{0.27}\text{Gd}_{0.74})_{3-w}\text{Mg}_w(\text{Ga}_{2.48}\text{Al}_{2.46})\text{O}_{12}$. The scintillators were prepared with a constant Ce content of 1% and a Mg content of 0 and 700 ppm, respectively. The Mg content is related to the Lu + Gd content. Further data is in Table 1. The films were prepared in the Technology Laboratory of Charles University, Prague, by isothermal dipping liquid phase epitaxy (LPE) (Kucera & Prusa, 2017). The films were grown from the $\text{BaO}-\text{B}_2\text{O}_3-\text{BaF}_2$ flux and deposited onto (100) oriented GGAG ($\text{Gd}_3\text{Ga}_3\text{Al}_2\text{O}_{12}$) Czochralski-grown substrates of 13 mm in diameter as demonstrated in Figure 2. The film thicknesses were determined by weighing. The composition was determined by electron probe micro-analysis (EPMA) and the Mg content by glow discharge mass spectrometry (GDMS).

For comparison, two reference standard single crystal scintillators were used. The first was a YAG:Ce scintillator and the second was a YAP:Ce scintillator, both produced in Crytur Ltd. These standard single crystals were grown with the Czochralski method and subsequently cut and polished into a 10 mm diameter and 1 mm thick disc.

In order to prevent the specimen surface from being electrically charged, and in order to conduct and measure an excitation current during electron beam characterization, each specimen was coated with a thin Al film with a thickness of 50 nm. The Al film also helps to increase the optical reflectivity to improve CL photon collection. The Al coating was deposited in a radiofrequency (RF) sputtering unit with 150 mm cathodes in the RF mode. Reactive sputtering was performed in argon and argon-oxygen atmospheres, respectively. The argon and oxygen fluxes were regulated with high accuracy by mass-flow controllers. The thickness was tested and calibrated using the Talystep surface profilometer.

TABLE 1 The description of the new ($\text{LuGAGG}:\text{Ce},(\text{Mg})$) LPE scintillators. The chemical formula of both samples is $(\text{Ce}_{0.01}\text{Lu}_{0.27}\text{Gd}_{0.74})_{3-w}\text{Mg}_w(\text{Ga}_{2.48}\text{Al}_{2.46})\text{O}_{12}$, w is shown in the table

Scintillator	Thickness (μm)	w	Mg conc. (ppm)
LuGAGG:Ce	16.3	0	0
LuGAGG:Ce,Mg	16.7	200×10^{-5}	700

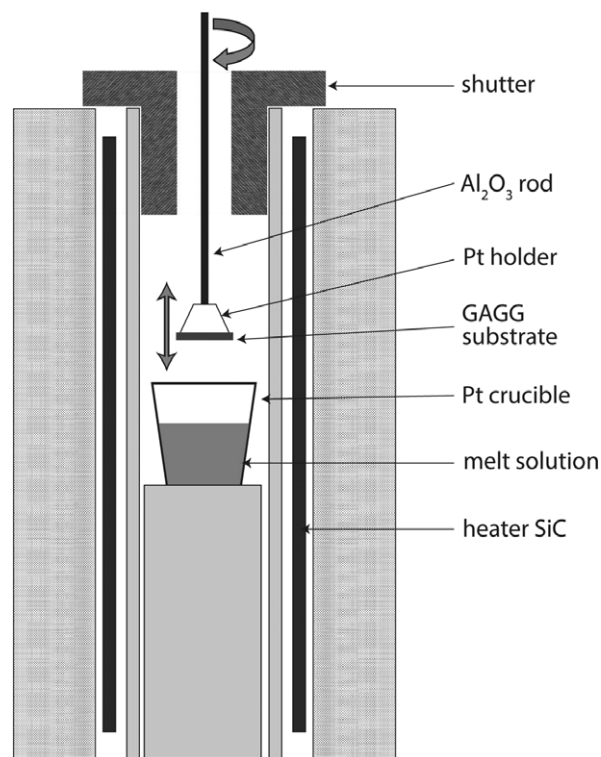


FIGURE 2 Schematic drawing of the apparatus for the preparation of isothermal LPE film scintillators

2.2 | Monte-Carlo simulation of absorbed electron energy

To determine the volume of electron beam interaction in scintillators, the a Monte-Carlo (MC) simulation was used. The simulation used allowed not only the determination of the maximum depth of electron penetration, but also the distribution of deposited excitation electrons during penetration. The MC model was based on the single scattering utilizing the screened Rutherford cross-section and the Bethe slowing down approximation. Also secondary processes associated with the diffusion of excited electrons were included in the model. The algorithms used were compiled for OS Windows as an application called "SCATTER" (Schauer & Bok, 2013). The perpendicular impact of electrons was simulated in this article, but it is not a problem to simulate an inclined impact. Calculations were done for the different energies of the electron beam that interacted in the new $\text{LuGAGG}:\text{Ce},(\text{Mg})$ epitaxial garnet film scintillators and in the reference YAG:Ce and YAP:Ce single crystal scintillators.

2.3 | Cathodoluminescence characterization

The $\text{LuGAGG}:\text{Ce},(\text{Mg})$ single crystalline film scintillators and the reference single crystal ones were studied using the equipment for the study of cathodoluminescence (CL) properties built in our laboratory in Brno (Bok & Schauer, 2011, 2014a). With this instrument, schematically drawn in Figure 3, a collimated e-beam of 10 keV excited the investigated specimen and the CL emission was collected by a light-guide from the opposite side of the specimen. An e-beam current of 30 nA and a spot with the diameter of 2 mm were used at the continuous (unmodulated) mode.

The CL emission spectra were measured using a Horiba JY iHR 320 spectrometer equipped with a Hamamatsu R943-02 PMT. The CL spectra were corrected for the spectral response of the apparatus. To study CL decay, the e-beam was periodically deflected out of an aperture in order to create e-beam pulses with a repetition rate of 1 kHz and a pulse width of 50 ns. In the pulsed mode, an e-beam current pulse of 150 nA and a beam spot diameter of 2 mm were used. To study spectrally unresolved decay, instead of guiding the emitted light to the spectrometer, the light was directed to an ET Enterprises 9113WB PMT connected to a Tektronix DPO7254 oscilloscope. The spectrally unresolved CL decays were measured in the whole spectral region between 200 and 800 nm. Using this setup, the relative intensity of the CL emission was measured as a spectrally corrected PMT anode current.

2.4 | Modulation transfer function

To evaluate the performance of the SEM scintillation detector with the new LuGAGG:Ce,Mg single crystalline film scintillators as compared with the standard single crystal YAG:Ce and YAP:Ce scintillators, the modulation transfer function (MTF) was calculated utilizing

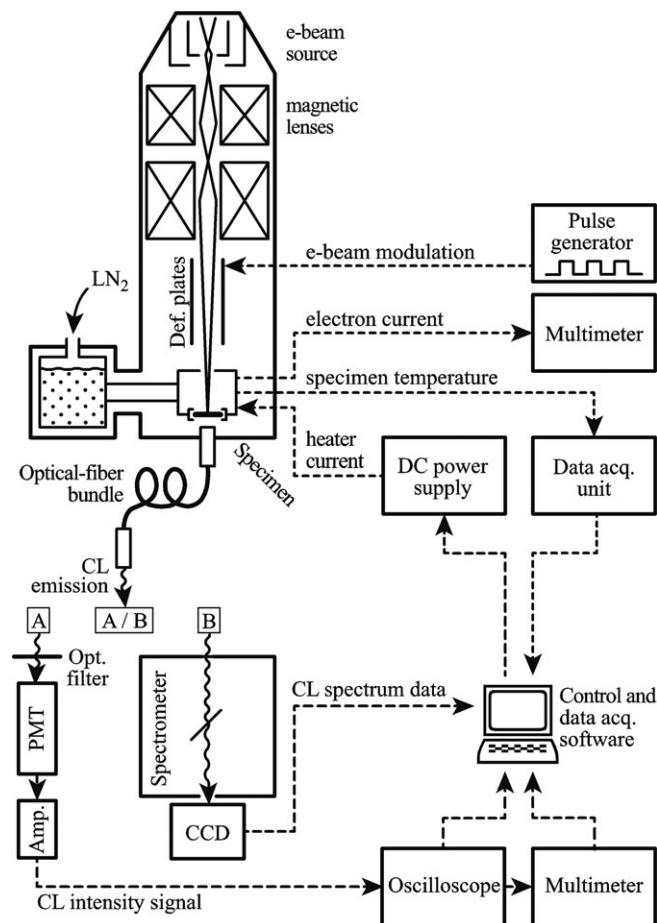


FIGURE 3 The block diagram of the equipment for the CL characterization of solids. The CL emission spectra were measured in the unmodulated mode using path B. The spectrally unresolved CL decays were measured in the pulsed mode using path A. Replacing an oscilloscope with a multimeter in path B the CL intensity was measured in the unmodulated mode

the method of scintillation rise and decay characteristics (Bok & Schauer, 2014b). For this purpose, the scintillators were excited by a 50 ns electron pulse using the spectrally unresolved experimental arrangement “A” in Figure 3. This represents the contrast transfer during the scanning with a dwell time of 50 ns.

2.5 | Optical characterization

The optical properties of the film scintillators and of the single crystal ones were obtained using the double-beam UV-VIS-NIR spectrophotometer Varian Cary 5. As with the LPE film growth the GGAG substrates were annealed with subsequent changes in color centers, measurements were made both in the reference sample mode and in the nonreference sample mode. In the case of the reference sample measurements, a suitably annealed substrate was used as the reference sample at the LPE film optical transmittance measurement. Reference samples of different thicknesses were used at the single crystal optical transmittance measurement. When measured without the reference sample, the obtained values were corrected to the reflectivity using the refractive index. The refractive indices for both films and single crystals were obtained with the minimum-deviation method (Kuwano, 1978; Kuwano, Saito, & Hase, 1988).

2.6 | Photon transport simulation

The SCIUNI Monte-Carlo (MC) simulation of photon transport in optical crystals was used to determine the efficiency of the light signal collection from a scintillator (Schauer, 2007). This method is based on the SCINTIL code for rotationally symmetric systems (Schauer & Atrata, 1992). This method makes use of the random generation of photon emission from a luminescent center about ten thousand times and describes the trajectory and the efficiency of the photon transport to the photocathode of the PMT. In fact, the value of the efficiency of each photon transport is given by the probability that the photon will reach the photocathode of the PMT. The result of the simulation is the signal transfer efficiency of the scintillation detector, depending on the location of the signal electron impact on the surface of the scintillator. The method enables the comparison of the efficiency of the scintillation detector according to the shape, size, and optical properties of the scintillator and the light guide.

3 | RESULTS AND DISCUSSION

3.1 | Electron interaction volumes

Replacing a standard bulk single crystal scintillator with a thin scintillation film in an electron detector in S(T)EM involves the risk that the penetration depth of the electrons will be greater than the thickness of the scintillation film. To predict this risk, the distribution of the absorbed electron energy in the penetration direction was investigated primarily in the new LuGAGG:Ce,(Mg) single crystalline films that have a thickness of about 16.5 μm , as described in Section 2.1. The energy distribution in the new film scintillators were compared with that in the standard bulk single crystal YAG:Ce scintillator. The results for the 10 and 20 keV primary electrons are shown in Figure 4.

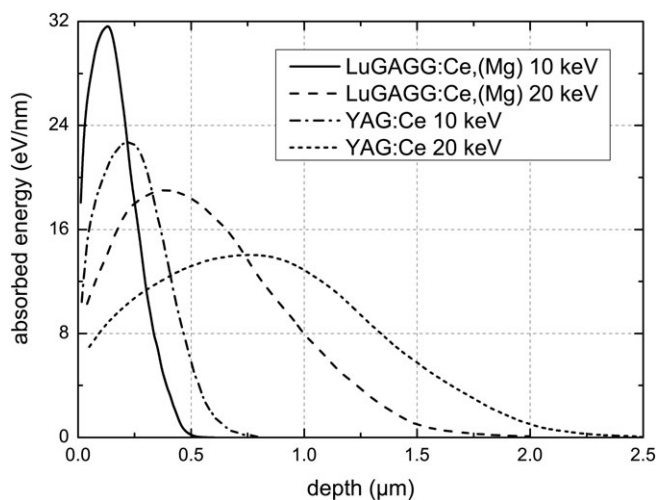


FIGURE 4 The Monte Carlo simulation of the electron absorbed energy distribution in the LuGAGG:Ce and LuGAGG:Ce,Mg film scintillators and in the standard YAG:Ce single crystal scintillator, all for the primary electron beam of 10 and 20 keV, respectively

The MC simulation method described in Section 2.2 was used to determine the presented dependence of the absorbed energy on the depth of the electron penetration in Figure 4. Also 3D electron trajectories and the dependence of the transversal distribution of the energy deposited by the excited electrons can be determined using this simulation (Schauer & Bok, 2013). However, the electron trajectories have little predictive value for the energy distribution, so they are unusable to determine losses due to electron passage through the film. The transversal distribution also has no significance in this case, because the diameter of the scintillators is large enough and the same for the both film and bulk scintillators. It is clear from the results in Figure 4 that, due to the small penetration depth of less than 1 μm for 10 keV electrons, which is the typical energy for the most scintillation detectors in S(T)EM, all energy is deposited in the 16.5 μm LuGAGG:Ce,(Mg) film and the GGAG substrate is not excited. It is, therefore, apparent that the new film scintillators may be even more than 10 times thinner than those studied.

3.2 | Electron-photon conversion

To investigate the performance of the scintillation detector for S(T)EM, an examination of electron-photon conversion is key, because this conversion fundamentally affects the MTF of the entire imaging system. The investigation includes a study of (1) the CL kinetics, (2) the energy conversion efficiency, and (3) the CL emission spectrum of the scintillator. The CL kinetics of the scintillator significantly affects the detector bandwidth (especially given the scintillator time response), which is the key to good MTF.

In order to evaluate the CL kinetics of the new LuGAGG:Ce,(Mg) scintillation films and to compare them with that of the standard single crystal YAG:Ce and YAP:Ce scintillators, the CL decay characteristics of the scintillators were measured at room temperature as described in Section 2.3. The measurement results that were corrected for the pulse width and for the instrument response function (IRF) are shown in Figure 5. Fittings of the experimental decay curves were carried out

assuming the presence of tunneling recombination using the sum of exponential and power functions (Schauer et al., 2017). The presented decay characteristics are normalized to unity at the beginning of the decay. Such a graphical representation with a dynamic range of decay intensities to four orders of magnitude allows for the determination of both the scintillator decay times (i.e., time when the intensity drop to $1/e$) and the values of their afterglows.

The values of the decay times and of the afterglows (1 and 5 μs after excitation) of the new LuGAGG:Ce,(Mg) scintillation films and of the standard single crystal YAG:Ce and YAP:Ce scintillators are shown in Table 2, together with the other electron-photon conversion quantities which are relevant for the imaging properties of the scintillators. It can be seen that the LuGAGG:Ce,Mg film exhibits a rapid decrease of its CL decay time to the value of 28 ns, compared with the Mg undoped LuGAGG:Ce specimen, which has the value of 61 ns. At the same time there is a significant reduction in the afterglow of the Mg co-doped film, even to the excellent value of 0.02% (1 μs after excitation), compared with the value of 0.13% for the Mg undoped film. As previously expressed in introductory Section 1, in S(T)EM imaging systems, the afterglow must be low even at the microsecond time range (after the excitation), which the new film scintillators meet. Compared with the standard single crystal YAG:Ce scintillators, which exhibit the decay time and afterglow (1 μs after excitation) 85 ns and 0.8%, respectively, all studied films provide a significant improvement in the CL decay kinetics.

In order to evaluate the efficiency and optical coupling of the new LuGAGG:Ce,(Mg) scintillation films, and to compare them to those of the standard single crystal YAG:Ce and YAP:Ce scintillators, their CL emission spectra, including the CL relative intensities, were measured as described in Section 2.3. The spectra were measured in the wavelength range from 200 to 800 nm at room temperature, and subsequently they were corrected for device spectral transmittance and for detector spectral sensitivity. Such processed spectra are shown in Figure 6. In order to assess the spectral matching of the new film scintillators to PMT photocathodes, the sensitivity spectra of the most common SbCs (S11) and multialkali (S20) photocathodes were

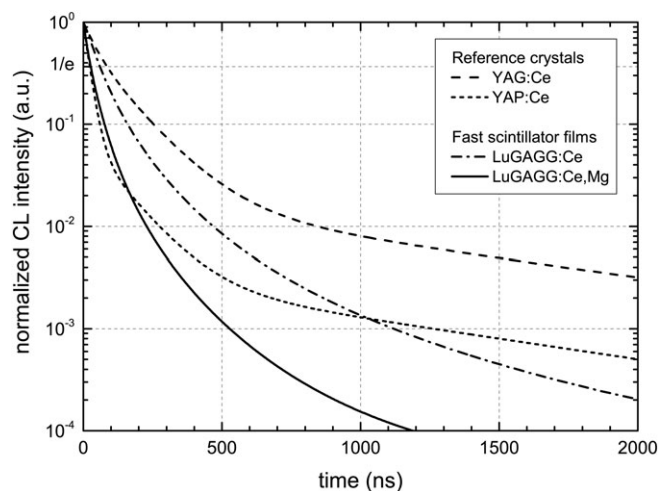


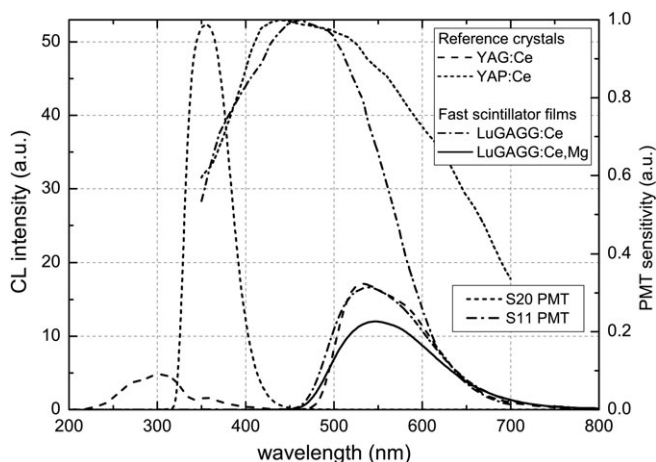
FIGURE 5 Cathodoluminescence decay characteristics of the LuGAGG:Ce and LuGAGG:Ce,Mg film scintillators and of the standard YAG:Ce and YAP:Ce single crystal scintillators

TABLE 2 Relevant imaging properties of the LuGAGG:Ce and LuGAGG:Ce,Mg film scintillators and of the standard YAG:Ce and YAP:Ce reference single crystal scintillators

Scintillators	Material form	Light yield ^b (p/keV)	Decay time (ns)	Afterglow at 1 μ s (%)	Afterglow at 5 μ s (%)	λ of max. emission (nm)
YAG:Ce	Single crystal	19	85	0.81	0.27	540
YAP:Ce	Single crystal	18	24	0.13	0.083	350
LuGAGG:Ce	Film ^a	20	61	0.13	<0.001	540
LuGAGG:Ce,Mg	Film ^a	15	28	0.02	<0.001	546

^a Single crystalline film.

^b Obtained using the YAG:Ce reference light yield value of 19 photons per keV electron.

**FIGURE 6** The cathodoluminescence (CL) emission spectra (left axis) of the LuGAGG:Ce and LuGAGG:Ce,Mg film scintillators and of the standard YAG:Ce and YAP:Ce single crystal scintillators, together with the standard PMT photocathode sensitivities (right axis)

measured and the results are also shown in Figure 6. The values of the maximum intensity wavelengths of the new LuGAGG:Ce, (Mg) scintillation film characteristic emissions and of the standard single crystal YAG:Ce and YAP:Ce scintillators are shown in Table 3. It is irrelevant that the Mg co-doped LuGAGG:Ce film has its CL emission maximum at about 546 nm, while the other garnet scintillators are near 540 nm. It is more significant that only Ce^{3+} -related 5d-4f emission is seen in the CL spectra of the studied LuGAGG:Ce,(Mg) epitaxial films in Figure 6.

Comparing the intensity of the characteristic emission peaks in Figure 6, it is clear that the LuGAGG:Ce film and the YAG:Ce single crystal scintillator have approximately the same energy conversion (CL) efficiency. Although the characteristic CL intensity of LuGAGG:Ce,Mg slightly increases with the increase of Mg concentration up to tens of ppm, unfortunately a further increase of Mg

co-doping above 280 ppm quenches the characteristic Ce^{3+} emission (Schauer et al., 2017). Such an effect has also been already noticed both in GAGG:Ce,Mg (Yoshikawa et al., 2016) and LuAG:Ce,Mg single crystals (Nikl et al., 2014) and also in ceramics (Liu et al., 2016). In any case, the CL efficiencies of the all garnet scintillators differ only insignificantly. The great advantage of all garnet scintillators is their CL characteristic emission in the wavelength range near 540 nm, which greatly expands the choice of a suitable cheap PMT. It should be noted that the YAP:Ce single crystal has its maximum emission at 350 nm, and although it has the higher CL efficiency, it can easily be lost on the PMT photocathode.

3.3 | Other relevant imaging properties

Other important properties of the scintillation detector based on the new LuGAGG:Ce,(Mg) film scintillators studied in this article are: (1) the MTF of the scintillator (and also of the detector); (2) the optical properties of the scintillator, of the light guide, and of the optical coupling components, including PMT matching; and (3) the simulation of the photon transport efficiency.

3.3.1 | Modulation transfer function

It has already been mentioned in this article that a good MTF of the scintillation detector is the key feature for the image quality of the objects studied in S(T)EM. Thus, the rise and decay characteristics of the new LuGAGG:Ce,(Mg) scintillation films, as well as of the standard single crystal YAG:Ce and YAP:Ce scintillators shown in Figure 5 and in Table 2, were used to calculate MTFs using the method described in Section 2.4 (Bok & Schauer, 2014b). The MTF calculation results are shown in Figure 7.

In this graph, MTF is plotted as a function of the spatial frequency expressed as a number of hypothetical line pairs per pixel (lp/pixel). It is obvious that the higher values of the spatial frequencies represent

TABLE 3 The significant optical parameters of the LuGAGG:Ce and LuGAGG:Ce,Mg film scintillators and of the standard YAG:Ce and YAP:Ce single crystal scintillators (λ is wavelength)

Scintillators	λ absorption (main peak) [nm]	λ absorption (minor peak) [nm]	λ char. CL emission [nm]	Absorption coeff. at λ_{emis} . [cm^{-1}]	Refraction index at λ_{emis} .	S20 PMT matching [%]	Photon trans. Eff. [%] ^b
YAP:Ce single crystal	290	210	355	1.61	1.990	60	40
YAG:Ce single crystal	456	336	540	0.74	1.837	73	48
LuGAGG:Ce,Mg film	437	341	546	0.58	1.845	72	See GAGG
GAGG substrate	n/a	n/a	n/a	0.43 ^a	1.843	n/a	56 ^c

^a Considered for the LuGAGG:Ce,Mg film peak.

^b Simulated for the matted output surface with no optical cement.

^c Simulated together with the LuGAGG:Ce,Mg film.

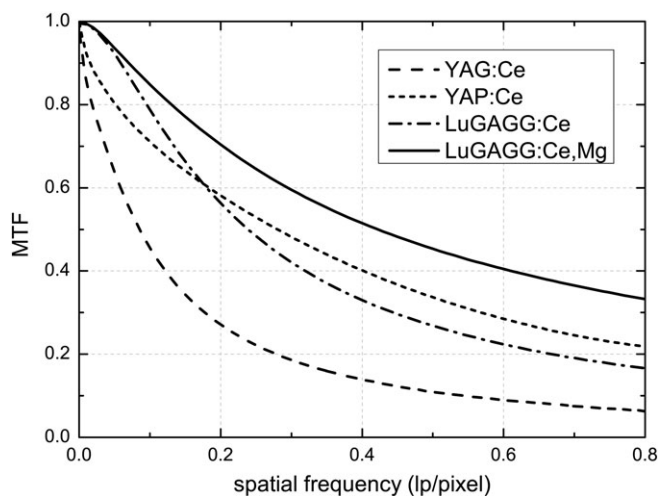


FIGURE 7 The spatial frequency dependence of the MTF of the LuGAGG:Ce and LuGAGG:Ce,Mg film scintillators as well as of the standard YAG:Ce and YAP:Ce single crystal scintillators in the S(T)EM scintillation detector. The time per pixel (dwell time) during the scanning was set to 50 ns

smaller object details. Ideal MTF has a value of 1, which guarantees the image transfer without a loss of contrast. Consequently, the larger the area under the curve, the better the contrast that is transferred to the resulting image by the scintillation detector. So, the best contrast transfer ability is shown by the scintillation detector with the LuGAGG:Ce,Mg film scintillator, and the worst ability is shown by the detector with the standard YAG:Ce single crystal scintillator. The spatial frequency dependence of MTF also shows that the YAG:Ce single crystal scintillator loses the contrast transfer ability at small details already above 0.1 lp/pixel, while the new LuGAGG:Ce,Mg film scintillator does so above 0.6 lp/pixel. This is related to the weak slow decay components of the LuGAGG:Ce,Mg film scintillator, whose influence on the image quality cannot be seen from the rise and decay characteristics.

3.3.2 | Optical properties

High optical self-absorption and/or the high refraction index of the scintillator can result in a significant loss of the efficiency of the entire scintillation detection system in S(T)EM. Therefore, the optical absorption coefficients of the new LuGAGG:Ce,(Mg) film scintillators and of their GGAG single crystal substrates were measured, and the results are shown in Figure 8. The refractive indices of the LuGAGG:Ce and LuGAGG:Ce,Mg film scintillators, of the YAG:Ce single crystal scintillator, and of the GGAG single crystal substrate were also determined, and the results are shown in Figure 9. The values of the relevant optical constants, together with the CL emission constants from Figure 6, are in Table 3.

Figure 8 shows that all of the studied scintillators exhibit significant optical absorption only outside the wavelength range of their characteristic CL emission. In the visible range of the spectrum, the absorption peak of the new LuGAGG:Ce and LuGAGG:Ce,Mg film scintillators is about four times higher than the absorption peak of the standard YAG:Ce single crystal scintillator. Optical absorption of the GGAG film substrate is very low in the entire measured spectral region from 250 to 550 nm, and almost without the peaks. However,

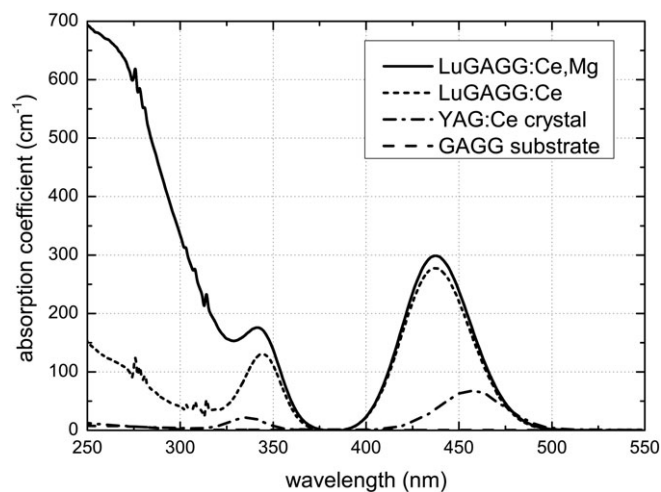


FIGURE 8 Optical absorption spectra of the LuGAGG:Ce and LuGAGG:Ce,Mg film scintillators, of their GGAG single crystal substrate, and of the standard YAG:Ce single crystal scintillator

in order to assess self-absorption, it is more important that the optical absorption coefficients of the studied films are very low in the range of their CL emission near 546 nm as shown in Table 3. Their self-absorptions are even lower than the self-absorption of the standard YAG:Ce single crystal scintillator with its CL emission near 540 nm. In other words, the studied films have a larger Stokes shift (i.e., the difference between absorption and emission peak positions) than the standard YAG:Ce single crystal, and this is a very advantageous property in terms of their self-absorption. Moreover, it is very important and advantageous that the optical absorption of the GGAG substrate is the lowest. Therefore, the LuGAGG:Ce,(Mg) film on the GGAG substrate can exhibit a significantly higher photon collection efficiency than the standard YAG:Ce single crystal, since the photon paths in the film are much shorter than that in the bulk scintillator.

The high refractive indices of the studied scintillators may critically deteriorate the photon escapes from the scintillators due to the low critical angles for the total reflection. Fortunately, the refractive

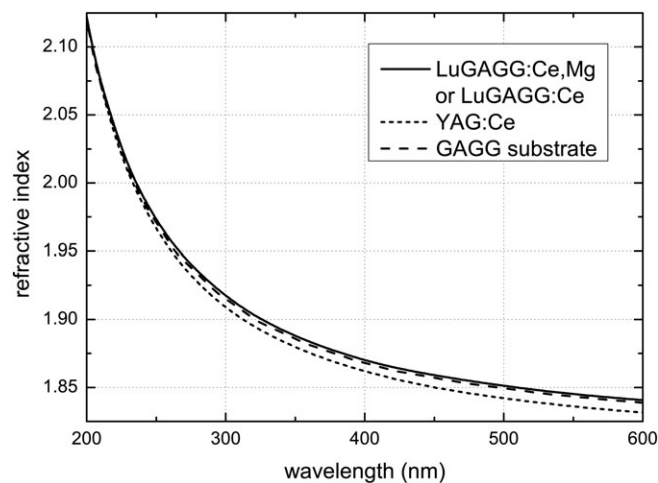


FIGURE 9 The wavelength dependence of the refractive indices of the LuGAGG:Ce and LuGAGG:Ce,Mg film scintillators, of their GGAG single crystal substrate, and of the standard YAG:Ce single crystal scintillator

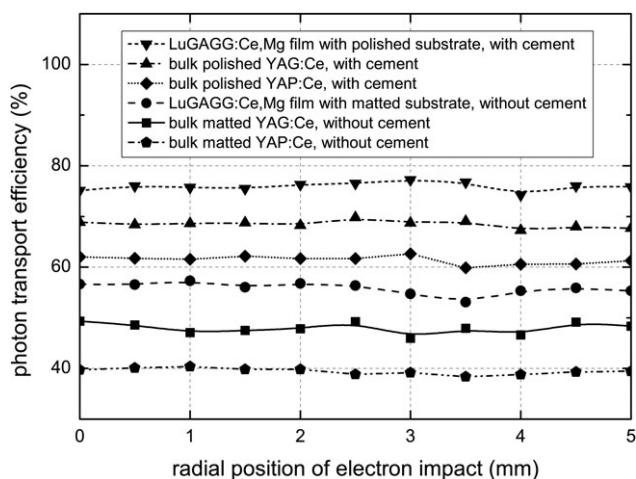


FIGURE 10 The simulated transport efficiency of signal photons in dependence on the radial position of the electron impact on the disk scintillator surface. The zero position corresponds to the center of the scintillator and the 5 mm position is at the edge of the scintillator. The photon transport efficiency was simulated only through the scintillator without any light guide

index magnitudes are important only in the spectral region of the CL emission of the studied scintillators (i.e., around the wavelength of about 540 nm). And, in this range, the refractive indices of the studied scintillators are relatively low, as seen in Figure 9. It is also possible to see that the refractive indices of all of the studied garnet scintillators and of the GGAG substrate are nearly the same. It follows that all the scintillators studied have nearly the same application potential in this respect.

Bad spectral matching of the scintillators to a PMT photocathode can significantly reduce the efficiency of the scintillation detector. Therefore, using the spectra in Figure 6, the spectral matching of the studied LuGAGG:Ce,Mg film scintillator and of the standard YAG:Ce and YAP:Ce single crystal ones to the multialkali (S20) photocathode was calculated and summarized in Table 3. It follows from the presented results that all of the garnet scintillators possess approximately the same matching to the multialkali photocathode, while the YAP:Ce single crystal shows the worst. However, the spectral matching of YAP:Ce could be markedly increased by using the PMT with the quartz entrance window. It is not the photocathode itself but the glass entrance window that causes the low spectral sensitivity of PMT in the short wave spectrum region. Unfortunately, the alternative with the quartz window increases the cost of the scintillation detector.

3.3.3 | Photon transport efficiency

These results for the optical parameters of the new LuGAGG:Ce,(Mg) scintillators allow us to qualify the problem of signal photon utilization in the scintillation detection system. But to quantify this problem, these optical parameters and the size and shape of the film scintillators and of all of the light-guiding components are only calculation parameters. If the quantification of the transport efficiency of the signal photons should be more than an imperfect estimate, then 3D calculations must be performed. As described in the introductory Section 1, the MC simulation is preferred for the quantification. The

results of the MC simulation performed by the method described in Section 2.6 are shown in Figure 10.

The MC simulation of the transport efficiency of signal photons was done only for the scintillators without any light guides in order to exclude losses in the light guides. In general, the light guides can destroy the scintillator's performance. Disk shape scintillators with a diameter of 10 mm and a thickness of 1 mm were simulated. The impact surface of all scintillators was simulated as Al coated with an internal reflectivity of 80%. The scintillator output surface was simulated either as matted (coupled without any optical cement) or as polished (coupled using the optical cement). If the optical cement was used, its absorption coefficient was set to 0.012 cm^{-1} and the refractive index to 1.56. The efficiency of each scintillator was simulated at 10 different signal electron impact points at the scintillator surface, equally spaced radially from the scintillator center (i.e., the zero position) to its edge at the 5 mm position in accordance with the earlier methodology (Schauer & Atrata, 1992). This is important when simulating more complicated scintillator shapes, but, as can be expected, the efficiency is essentially independent of the signal electron impact position for the disk-shaped scintillator. The differences in the individual positions are given only by statistical deviations so the efficiency can be expressed as the only constant value. This value is reported in Table 3 as the mean value from the data for the matted scintillator output with no optical cement in Figure 10. The simulated results of the photon transport efficiency show a non-negligible increase in the detector efficiency for all of the film-substrate garnet scintillators compared with the bulk single crystal ones. This efficiency improvement of about 8% is due to the lower self-absorption in the film-substrate scintillator. This will be discussed in more detail together with the evaluation of the polished scintillators in Section 3.4.

3.4 | Discussion of results

As is evident from the results above, a significant improvement in the performance of the current scintillation electron detectors for S(TEM) is possible. However, it is not possible to quantify the improvement and assess the potential of the detector without an MTF evaluation. The presented comparison of the MTFs of the new prospective LuGAGG:Ce,Mg film scintillators with the MTFs of the standard YAG:Ce single crystal ones shows that it is possible to achieve up to six times better resolution for significant details with the faster film scintillators at the same contrast. This proves that finding and testing faster scintillators is crucial for detector quality.

The presented results of the electron-photon conversion of the LuGAGG:Ce,Mg film scintillators show that a strategy to get significantly faster CL decays of scintillators can be based on the creation of an additional fast radiative recombination pathway, which would efficiently compete in electron trapping from the conduction band with the shallow electron traps in the garnet hosts (Kucera et al., 2016). To ensure such fast recombination in garnet scintillators, the stabilization of tetravalent Ce^{4+} centers in the garnet lattice by divalent rare earth ion co-doping was realized (Nikl et al., 2014).

Moreover, a different technology of LuGAGG:Ce,Mg film scintillator preparation (compared with that of single crystal Czochralski growth) contributes to the faster recombination in the film

scintillators. This is because the lower preparation temperature during the growth of the LPE films is the main cause of the antisite defect absence. Unlike LPE films, Czochralski-grown single crystal garnets possess antisite defects that are responsible for the broad UV CL emission at 250–400 nm in Figure 6. These antisite defects are also responsible for the slow CL decay components in the standard YAG:Ce single crystal scintillators, and above all for their high afterglow in the microsecond time range in Figure 5. Developers of scintillation electron detectors for S(T)EM have been faced with this problem for many years (Autrata & Schauer, 1995; Schauer, 2011).

The excellent result of both of the mentioned defect engineering approaches is the significant CL decay reduction with the use of the LuGAGG:Ce,Mg film scintillators, as presented in Figure 5. Specifically, the afterglow at the microsecond time range is considerably suppressed, which is very important for the very fast imaging in the S(T)EM detectors operating at high-rate conditions. Although the Mg²⁺ co-doping of the LuGAGG:Ce multicomponent garnets does not favorably affect the electron–photon conversion efficiency presented in Figure 6, the important fact is that the considerable CL temperature quenching of the studied LuGAGG:Ce,Mg film scintillator begins at approximately the temperature of 300 K, that is, above room temperature as previously published (Schauer et al., 2017). Similar results were also reported by photoluminescence studies of other multicomponent garnets (Chewpraditkul et al., 2014, 2016). The LuGAGG:Ce,Mg film scintillators may be useful even in an environment with a considerably higher temperature, because they show at least 50% of the low temperature intensity up to the temperature of 400 K.

The small scintillator thickness is a drawback for many scintillation radiation detectors where a high penetration depth of radiation is a problem, but the LuGAGG:Ce,(Mg) film with a thickness of 16.5 μm is no problem for any S(T)EM scintillation electron detector because the penetration depth for the typical signal electrons in S(T)EM of 10 keV is less than 1 μm, as demonstrated in Figure 4, and the self-absorption of the signal photons is low.

As for the transport efficiency of the signal photons, it should be noted that the 3D photon trajectories in the scintillator are much longer than the thickness of the scintillator (both bulk scintillator and the film-substrate one). And not only this, an important effect on the transport efficiency is also the photon escape from the scintillator, which is determined by the refractive index of the scintillator. Therefore, the differences in the photon transport efficiency in different scintillators are much higher than can be estimated from the optical parameters listed in Table 3. This is evidenced from the results of the photon transport MC simulation in the very simple symmetric disk scintillator in Figure 10. For such shaped scintillator, the simulated photon transport efficiency of 56% for the LuGAGG:Ce,Mg-GAGG (film-substrate) scintillator is even 8% higher than that for the bulk standard YAG:Ce one. In addition, improving the photon transport in the system with the film–substrate scintillator is highly dependent on the geometry of the scintillation detector. So, for more complex BSE detectors the increase of the photon transport efficiency in the LuGAGG:Ce,Mg based detector may be even higher.

It is true that the simulated results of the photon transport efficiency in Figure 10 show that the polished alternative with the optical cement has the highest efficiency, but such an alternative has a

disadvantageous effect on the efficiency of the system with the light guide. This is because the matted scintillator output without cement reduces the loss of photon through the light-guide sidewalls. Therefore, the polished alternative with the optical cement is not commonly used. In any case, the LuGAGG:Ce,Mg film (with the polished output using the optical cement) efficiency of 76% in Figure 10 is by far the best value ever reported for disk-shaped scintillators.

It is difficult to assess the production costs of the film scintillators for the time being because the studied scintillators were prepared in the academic laboratory, and the commercial production of the film scintillators has not yet been mastered. However, it can be estimated that the production of the standard single crystal scintillators will be cheaper, since the growth of the films is not possible without the production of the single crystal substrates.

4 | CONCLUSION

The performance of the scintillation electron detectors for S(T)EM based on the new scintillation garnet films was studied in this article. Two LuGAGG:Ce,(Mg) epitaxial garnet film scintillators were prepared to study their electron interaction volumes, cathodoluminescence (CL) properties, and optical properties. Using the results of this study, the MTF of the scintillation detector based on the mentioned garnet film was calculated and compared with the MTF of the detector based on the standard bulk single crystal YAG:Ce and YAP:Ce scintillators. Beside this, the MC simulation of the photon transport efficiency of film scintillators was determined and compared with the efficiency of the standard bulk scintillators.

It was found that a significant improvement is possible in the performance of the current standard scintillation electron detectors for S(T)EM based on the standard bulk single crystal YAG:Ce or YAP:Ce scintillator. The presented results show that the LuGAGG:Ce,Mg film scintillators have excellent electron–photon conversion parameters. They possess significantly faster CL decays compared with the current standard single crystal YAG:Ce scintillators. This happens due to the creation of an additional fast radiative recombination pathway, which would efficiently compete in electron trapping from the conduction band with the shallow electron traps in the garnet hosts. In such a case, the stabilization of tetravalent Ce⁴⁺ centers in the garnet lattice by divalent rare earth ion co-doping is accomplished. Also the lower preparation temperature during the growth of the LPE films, when the antisite defects are avoided, contributes to the faster recombination in the film scintillators. Therefore, the studied LuGAGG:Ce,Mg films exhibit a very short CL decay time of 28 ns and an afterglow of only 0.02%.

Very important are the results that describe the ability to show fine image details with the detectors based on the LuGAGG:Ce,Mg film scintillators utilizing the MTF calculation. This is the key to a good image with high contrast in S(T)EM. The presented comparison of the MTF of the new prospective LuGAGG:Ce,Mg film scintillators with that of the standard YAG:Ce single crystal scintillator shows that using the film scintillators a resolution for significant details up to six times higher can be achieved in S(T)EM at the same contrast. This result

proves that finding and applying faster scintillators is crucial for detector quality.

Although the shape and size of the scintillator, its optical self-absorption, refractive index, and other optical properties are often omitted when evaluating the performance of the scintillation electron detectors for S(T)EM, the MC simulation results presented in this article show that these properties have a notable effect on the performance of the detector. The MC simulation of the photon transport efficiency in the film-substrate scintillator, as well as in the bulk one, shows that there are large differences in optical performance even among scintillators with a very simple symmetrical shape. In such a case, the new prospective LuGAGG:Ce,Mg film scintillator with the GAGG substrate has an 8% higher transport efficiency of the signal photons than the standard bulk YAG:Ce single crystal one.

In summary, the significantly improved MTF, the satisfying electron-photon conversion efficiency, and the higher transport efficiency of the signal photons predetermines LuGAGG:Ce,Mg film scintillators for an application in very fast scintillation electron detectors, not only in S(T)EM but also in other e-beam devices.

ACKNOWLEDGMENTS

This research was supported by the Czech Science Foundation (projects GA16-05631S and GA16-15569S) and by the Ministry of Education, Youth and Sports of the Czech Republic (project LO1212). The research infrastructure was funded by the Ministry of Education, Youth and Sports of the Czech Republic and European Commission (project CZ.1.05/2.1.00/01.0017) and by the Czech Academy of Sciences (project RVO:68081731).

ORCID

Petr Schauer  <https://orcid.org/0000-0002-7930-0983>

REFERENCES

Autrata, R., & Schauer, P. (1995). Cathodoluminescent properties of single crystal materials for electron microscopy. *Scanning Microscopy*, 9, 1–12.

Autrata, R., Schauer, P., Kvapil, J., & Kvapil, J. (1978). A single crystal of YAG-new fast scintillator in SEM. *Journal of Physics E: Scientific Instruments*, 11, 707–708.

Autrata, R., Schauer, P., Kvapil, J., & Kvapil, J. (1983a). Cathodoluminescent efficiency of Y3Al5O12 and YAlO3 single crystals in dependence on Ce3+ and other dopants concentration. *Crystal Research and Technology*, 18, 907–913.

Autrata, R., Schauer, P., Kvapil, J., & Kvapil, J. (1983b). Single-crystal aluminates—a new generation of scintillators for scanning electron microscopes and transparent screens in electron optical devices. *Scanning Electron Microscopy*, 2, 489.

Autrata, R., Schauer, P., Kvapil, J., & Kvapil, J. (1983c). A single crystal of YAlO3: Ce3+ as a fast scintillator in SEM. *Scanning*, 5, 91–96.

Bok, J., Lalinský, O., Hanuš, M., Onderišinová, Z., Kelar, J., & Kučera, M. (2016). GAGG: Ce single crystalline films: New perspective scintillators for electron detection in SEM. *Ultramicroscopy*, 163(1–5), 1–5.

Bok, J., & Schauer, P. (2011). LabVIEW-based control and data acquisition system for cathodoluminescence experiments. *Review of Scientific Instruments*, 82, 113109.

Bok, J., & Schauer, P. (2014a). Apparatus for temperature-dependent cathodoluminescence characterization of materials. *Measurement Science and Technology*, 25, 075601.

Bok, J., & Schauer, P. (2014b). Performance of SEM scintillation detector evaluated by modulation transfer function and detective quantum efficiency function. *Scanning*, 36, 384–393.

Carrier, C., & Lecomte, R. (1990). Theoretical modeling of light transport in rectangular Parallelepipedic scintillators. *Nuclear Instruments & Methods in Physics Research Section A-Accelerators Spectrometers Detectors and Associated Equipment*, 292, 685–692.

Danilatos, G. D. (2012). Backscattered electron detection in environmental SEM. *Journal of Microscopy*, 245, 171–185.

Filippov, M. N., Rau, E. I., Sennov, R. A., Boyde, A., & Howell, P. G. T. H. (2001). Light collection efficiency and light transport in backscattered electron scintillator detectors in scanning electron microscopy. *Scanning*, 23, 305–312.

Hibino, M., Irie, K., Autrata, R., & Schauer, P. (1992). Characteristics of Yag single-crystals for electron scintillators of Stem. *Journal of Electron Microscopy*, 41, 453–457.

Chewpraditkul, W., Bruza, P., Panek, D., Pattanaboonmee, N., Wantong, K., Chewpraditkul, W., ... Nikl, M. (2016). Optical and scintillation properties of Ce3+-doped YGd2Al5-xGaxO12 (x=2,3,4) single crystal scintillators. *Journal of Luminescence*, 169, 43–50.

Chewpraditkul, W., Panek, D., Bruza, P., Chewpraditkul, W., Wanarak, C., Pattanaboonmee, N., ... Nikl, M. (2014). Luminescence properties and scintillation response in Ce3+-doped Y2Gd1Al5-xGaxO12 (x=2, 3, 4) single crystals. *Journal of Applied Physics*, 116, 083505.

Chewpraditkul, W., Swiderski, L., Moszynski, M., Szczesniak, T., Syntfeld-Kazuch, A., Wanarak, C., & Limsuwan, P. (2009). Scintillation properties of LuAG: Ce, YAG: Ce and LYSO: Ce crystals for gamma-ray detection. *IEEE Transactions on Nuclear Science*, 56, 3800–3805.

Keil, G. (1970). Design principles of fluorescence radiation converters. *Nuclear Instruments and Methods*, 89, 111–123.

Kucera, M., Onderišinová, Z., Bok, J., Hanuš, M., Schauer, P., & Nikl, M. (2016). Scintillation response of Ce 3+ doped GdGa-LuAG multicomponent garnet films under e-beam excitation. *Journal of Luminescence*, 169, 674–677.

Kucera, M., & Prusa, P. (2017). Chapter 5: LPE-grown thin-film scintillators. In M. Nikl (Ed.), *Nanocomposite, ceramic and thin film scintillators* (pp. 155–226). Singapore: Pan Stanford Publishing.

Kuwano, Y. (1978). Refractive-indexes of YAlO3-Nd. *Journal of Applied Physics*, 49, 4223–4224.

Kuwano, Y., Saito, S., & Hase, U. (1988). Crystal-growth and optical-properties of Nd-Ggag. *Journal of Crystal Growth*, 92, 17–22.

Liu, S. P., Mares, J. A., Feng, X. Q., Vedda, A., Fasoli, M., Shi, Y., ... Nikl, M. (2016). Towards bright and fast Lu3Al5O12:Ce,mg optical ceramics scintillators. *Advanced Optical Materials*, 4, 731–739.

Nikl, M., Kamada, K., Babin, V., Pejchal, J., Pilarova, K., Mihokova, E., ... Yoshikawa, A. (2014). Defect engineering in Ce-doped aluminum garnet single crystal scintillators. *Crystal Growth & Design*, 14, 4827–4833.

Nikl, M., Vedda, A., Fasoli, M., Fontana, I., Laguta, V., Mihokova, E., ... Nejezchleb, K. (2007). Shallow traps and radiative recombination processes in Lu 3 Al 5 O 12: Ce single crystal scintillator. *Physical Review B*, 76, 195121.

Nikl, M., & Yoshikawa, A. (2015). Recent R&D trends in inorganic single-crystal scintillator materials for radiation detection. *Advanced Optical Materials*, 3, 463–481.

Nikl, M., Yoshikawa, A., Kamada, K., Nejezchleb, K., Stanek, C., Mares, J., & Blazek, K. (2013). Development of LuAG-based scintillator crystals—a review. *Progress in Crystal Growth and Characterization of Materials*, 59, 47–72.

Schauer, P. (1982). *Study of cathodoluminescence properties of YAG:Ce and YAP:Ce single crystals* (PhD Thesis). Brno University of Technology, Brno, Czech Republic.

Schauer, P. (2007). Extended algorithm for simulation of light transport in single crystal scintillation detectors for S(T)EM. *Scanning*, 29, 249–253.

Schauer, P. (2011). Optimization of decay kinetics of YAG: Ce single crystal scintillators for S (T) EM electron detectors. *Nuclear Instruments and Methods in Physics Research Section B: Beam Interactions with Materials and Atoms*, 269, 2572–2577.

Schauer, P., & Autrata, R. (1979). Electro-optical properties of a scintillation detector in Sem. *Journal De Microscopie Et De Spectroscopie Electroniques*, 4, 633–650.

- Schauer, P., & Atrata, R. (1992). Light transport in single-crystal scintillation detectors in SEM. *Scanning*, 14, 325–333.
- Schauer, P., & Bok, J. (2013). Study of spatial resolution of YAG: Ce cathodoluminescent imaging screens. *Nuclear Instruments and Methods in Physics Research Section B: Beam Interactions with Materials and Atoms*, 308, 68–73.
- Schauer, P., Lalinsky, O., Kucera, M., Lucenicova, Z., & Hanus, M. (2017). Effect of mg co-doping on cathodoluminescence properties of LuGAGG:Ce single crystalline garnet films. *Optical Materials*, 72, 359–366.
- Yamamoto, K., Tanji, T., Hibino, M., Schauer, P., & Atrata, R. (2000). Improvement of light collection efficiency of lens-coupled YAG screen TV system for a high-voltage electron microscope. *Microscopy Research and Technique*, 49, 596–604.
- Yoshikawa, A., Kamada, K., Kurosawa, S., Shoji, Y., Yokota, Y., Chani, V. I., & Nikl, M. (2016). Crystal growth and scintillation properties of multi-component oxide single crystals: Ce:GGAG and Ce:LaGPS. *Journal of Luminescence*, 169, 387–393.

How to cite this article: Schauer P, Lalinský O, Kučera M. Prospective scintillation electron detectors for S(T)EM based on garnet film scintillators. *Microsc Res Tech*. 2019;82: 272–282. <https://doi.org/10.1002/jemt.23169>